



# The Loss of Efficiency Caused by Agents' Uncoordinated Routing in Transport Networks

Zhongzhi Xu<sup>1</sup>, Li Sun<sup>1</sup>, Junjie Wang, Pu Wang\*

School of Traffic and Transportation Engineering, Central South University, Changsha, Hunan, P.R. China

## Abstract

Large-scale daily commuting data were combined with detailed geographical information system (GIS) data to analyze the loss of transport efficiency caused by drivers' uncoordinated routing in urban road networks. We used Price of Anarchy (POA) to quantify the loss of transport efficiency and found that both volume and distribution of human mobility demand determine the POA. In order to reduce POA, a small number of highways require considerable decreases in traffic, and their neighboring arterial roads need to attract more traffic. The magnitude of the adjustment in traffic flow can be estimated using the fundamental measure traffic flow only, which is widely available and easy to collect. Surprisingly, the most congested roads or the roads with largest traffic flow were not those requiring the most reduction of traffic. This study can offer guidance for the optimal control of urban traffic and facilitate improvements in the efficiency of transport networks.

**Citation:** Xu Z, Sun L, Wang J, Wang P (2014) The Loss of Efficiency Caused by Agents' Uncoordinated Routing in Transport Networks. PLoS ONE 9(10): e111088. doi:10.1371/journal.pone.0111088

**Editor:** Wen-Bo Du, Beihang University, China

**Received:** July 25, 2014; **Accepted:** September 27, 2014; **Published:** October 28, 2014

**Copyright:** © 2014 Xu et al. This is an open-access article distributed under the terms of the Creative Commons Attribution License, which permits unrestricted use, distribution, and reproduction in any medium, provided the original author and source are credited.

**Data Availability:** The authors confirm that all data underlying the findings are fully available without restriction. All the data in this study was obtained from NAVTEQ and Caliper Corporation. Requests for data can be sent to the following addresses: NAVTEQ Data Email: sales@korem.com Phone: 1 418 647-1555 330 St. Vallier Street East, Suite 240 Quebec (Quebec), Canada, G1K 9C5 Caliper Data Phone: +1 617-527-4700 E-mail: sales@caliper.com 1172 Beacon Street, Suite 300 Newton MA 02461-9926, USA.

**Funding:** The work is supported by the National Natural Science Foundation of China (No. 51208520), the FokYing Tong Education Foundation (No. 141075), and the Shenghua Scholar Program of Central South University. The funders had no role in study design, data collection and analysis, decision to publish, or preparation of the manuscript.

**Competing Interests:** The authors have declared that no competing interests exist.

\* Email: wangpu@csu.edu.cn

† These authors contributed equally to this work.

## Introduction

In this era of unprecedented global urbanization, the fast growth of human mobility has put immense pressure on urban roads [1–3], which has manifested in the form of severe traffic congestion and traffic-related air pollution [4–7]. Improving the efficiency of transport networks has become an urgent problem to solve and it has recently attracted widespread attention from scientific and engineering fields [8–14]. The transport efficiency of a road network is primarily determined by its network topology [15–21], by the volume and distribution of travel demand [9,18–20], and by drivers' routing behavior (the manner in which the road network is used) [11–14]. Studies have shown that increasing the capacity of the important backbone of transportation networks [10] or removing specific segments [11] can make these networks more efficient. It has also been discovered that traffic congestion can be mitigated efficiently by intelligently reducing a small fraction of travel demand [9].

Despite the intensive investigations on the effects of network topology and travel demand on the efficiency of transport networks, the effect of agents' routing behavior has only been studied on theoretical networks or simplified road networks, without considering actual travel demand [11–15]. Using three urban road networks, one type of transport networks, as an example, we show a comprehensive image of the loss of transport efficiency caused by agents' (drivers') uncoordinated routing. Furthermore, we explored the way that can lead a road network to

its optimal state. We also believe our findings can shed light on improving other types of transport networks experiencing a lack of coordination among agents, such as the Internet [22].

## Data and Methods

The road networks in San Francisco, Santa Clara, and Alameda were extracted from the Bay Area road network (Figure 1), which was provided by NAVTEQ, a commercial provider of geographical information systems data [23]. The road networks are composed of highways and arterial roads. There are 2,816 road segments in San Francisco, 7,269 in Santa Clara, and 5,805 in Alameda. There are 1,144 intersections in San Francisco, 3,420 in Santa Clara, and 2,744 in Alameda. More detailed information regarding the three road networks was provided in Table S1 and Figure S1.

In the following, the Bay Area commuting OD (origin-destination matrix) was first estimated, and consequently the commuting OD was calculated for each county. The Bay Area daily home-work commuting data were provided by the U.S. census bureau [24]. The numbers of trips from residents' home locations to work locations at a street-block level were recorded. The street blocks were grouped into census tracts where they were located (1,398 in total) for generating the census tract based OD.

People use various modes of transportation in their daily commutes, these include cars (driving alone), carpooling, public transportation, bicycling, and walking. Based on the mode split

data, the vehicle use rate was calculated for each census tract [25]:

$$VUR(i) = P_{driver}(i) + P_{carpool}(i) / S \quad (1)$$

Here,  $P_{driver}(i)$  and  $P_{carpool}(i)$  are the fractions of residents in census tract  $i$  who drive alone or share a car. The average carpool size in California ( $S = 2.25$ ) was used for these calculations [26]. Next, a mode of transportation (vehicle or non-vehicle) was randomly assigned to each of the residents of each census tract according to the estimated vehicle usage rate  $VUR$  (Figure S2). Then the trips not completed by vehicles were filtered out, generating the vehicle-based commuting OD.

The average number of daily trips per person is about 4 in the U.S., this generates about 22 million trips in the Bay Area [27]. Based on the daily distribution of traffic volume, average hourly trip production  $W$  during the morning commute (6:00 a.m.–10:00 a.m.) was estimated [28]. The vehicle-based daily commuting OD was rescaled using  $W$  to estimate the morning peak hourly commuting OD.

To assign trips to the road networks, the census tract based OD was mapped to the intersection-based OD. For each trip in the

census tract based OD, the road intersections within the origin census tract and destination census tract were identified (Figure S3). One intersection in the origin census tract and one intersection in the destination census tract were randomly selected as the origin and destination of the trip in the intersection-based OD.

Finally, the commuting ODs for the three road networks were extracted. Using San Francisco as an example, trips start and end within the county formalize the internal-internal OD, trips that start within the county and end outside it and trips start outside the county and end within it formalize the internal-external OD and the external-internal OD. Trips that start and end outside the county formalize the external-external OD. The origins and destinations of each internal-external trip, external-internal trip, and external-external trip were mapped to the San Francisco road network (Figure 2a). For each internal-external trip, the Dijkstra algorithm was used to find the shortest path (measured in travel time) within the Bay Area road network [29]. The destination of the trip was replaced with the last road intersection that the driver passed before leaving San Francisco. For each external-internal trip, the origin of the trip was mapped to the first road intersection



**Figure 1. Bay Area road network and locations of three counties.**  
doi:10.1371/journal.pone.0111088.g001

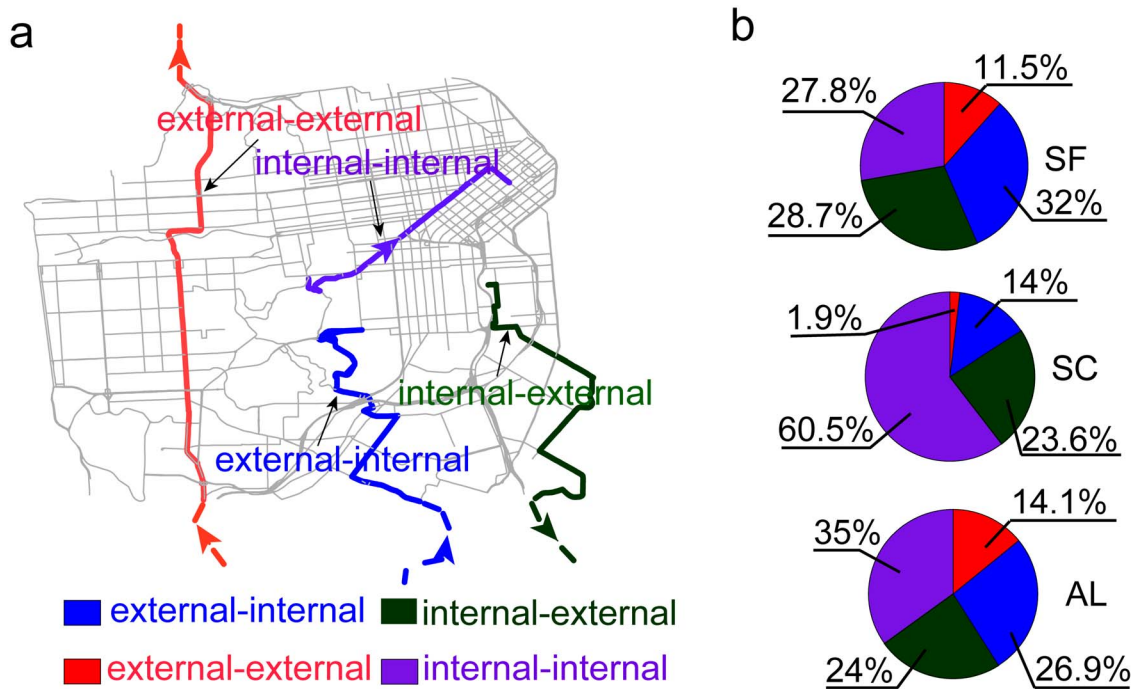


**Figure 2. Illustration and statistics of the four types of trips.** (a) Four types of trips defined by the locations of the origin and destination. Purple, green, blue, and red lines represent the path of an internal-internal trip, an internal-external trip, an external-internal trip, and an external-external trip respectively. (b) The statistics of the four types of trips in San Francisco (SF), Santa Clara (SC) and Alameda (AL) (also see Table S2). doi:10.1371/journal.pone.0111088.g002

that the driver passed upon entering San Francisco. For each external-external trip, the new origin and destination were mapped to the first road intersection that the driver passed upon entering San Francisco and the last intersection passed before leaving San Francisco. The four types of ODs were also generated for Santa Clara and Alameda.

Due to different geographic locations and patterns of land use, the four types of ODs showed different combinations in the three counties (Figure 2b). In San Francisco, there were similar numbers of internal-internal trips, internal-external trips, and external-internal trips. There were slightly more external-internal trips than internal-external trips, indicating that more people enter San Francisco during the morning peak. In Santa Clara, the majority of trips (60.5%) were within the county. There were many more people leaving than entering the county during the morning. People rarely drove across the county. In Alameda, although the majority of trips began and ended within the county, the number of internal-internal trips (35%) was only slightly higher than that of internal-external trips (24%) and external-internal trips (26.9%). Alameda had the most cross-county trips.

The number of trips between a pair of origin and destination  $N$  can be approximated by a power-law distribution  $P(N) = 509.2N^{-3.32}$  for all the three counties  $R^2 > 0.99$ , showing that travel demand between most pairs of locations was small, but there was high volume between a few origins and destinations (Figure 3d). The random OD, which had the same number of OD pairs and the same number of trips as the San Francisco OD, was generated and used for conducting comparative studies. The trips in the random OD were randomly assigned to pairs of origins and destinations.

### User Equilibrium and Social Optimum

Based on the ODs generated for the three road networks, traffic flow along each road segment was estimated under two scenarios. In the first scenario, all drivers were assumed to know all information regarding the road network and put their own interests first. In this scenario, the whole system reached the user equilibrium (UE) such that no driver could reduce travel time any further by switching paths. This is also known as the Nash equilibrium [12]. The second scenario was the social optimum (SO), the state that was most beneficial overall, meaning that it minimized the total travel time across the whole system [11,30]. The price of anarchy POA was then defined as the ratio of the total travel time of the Nash equilibrium and the total travel time of the social optimum:

$$POA = T_{UE} / T_{SO} \tag{2}$$

The price of anarchy POA quantifies the loss of transportation efficiency caused by drivers' selfish routing. Given the huge traffic volume in a big city, a small POA can still mean a big loss of efficiency. Understanding the method to reduce POA has important consequences for the optimal design and control of transportation systems.

To calculate the equilibrium flow  $f_{UE}$  under UE scenario, Wardrop's principle, as described by the Beckmann model, was used [31]. In this case, the objective function in Eq. (3) was minimized:

$$T_{UE} = \sum \int_0^{f_{ij}} t_{ij}(f) df \tag{3}$$

Here,  $f_{ij}$  and  $t_{ij}$  represent the traffic flow and travel time between a

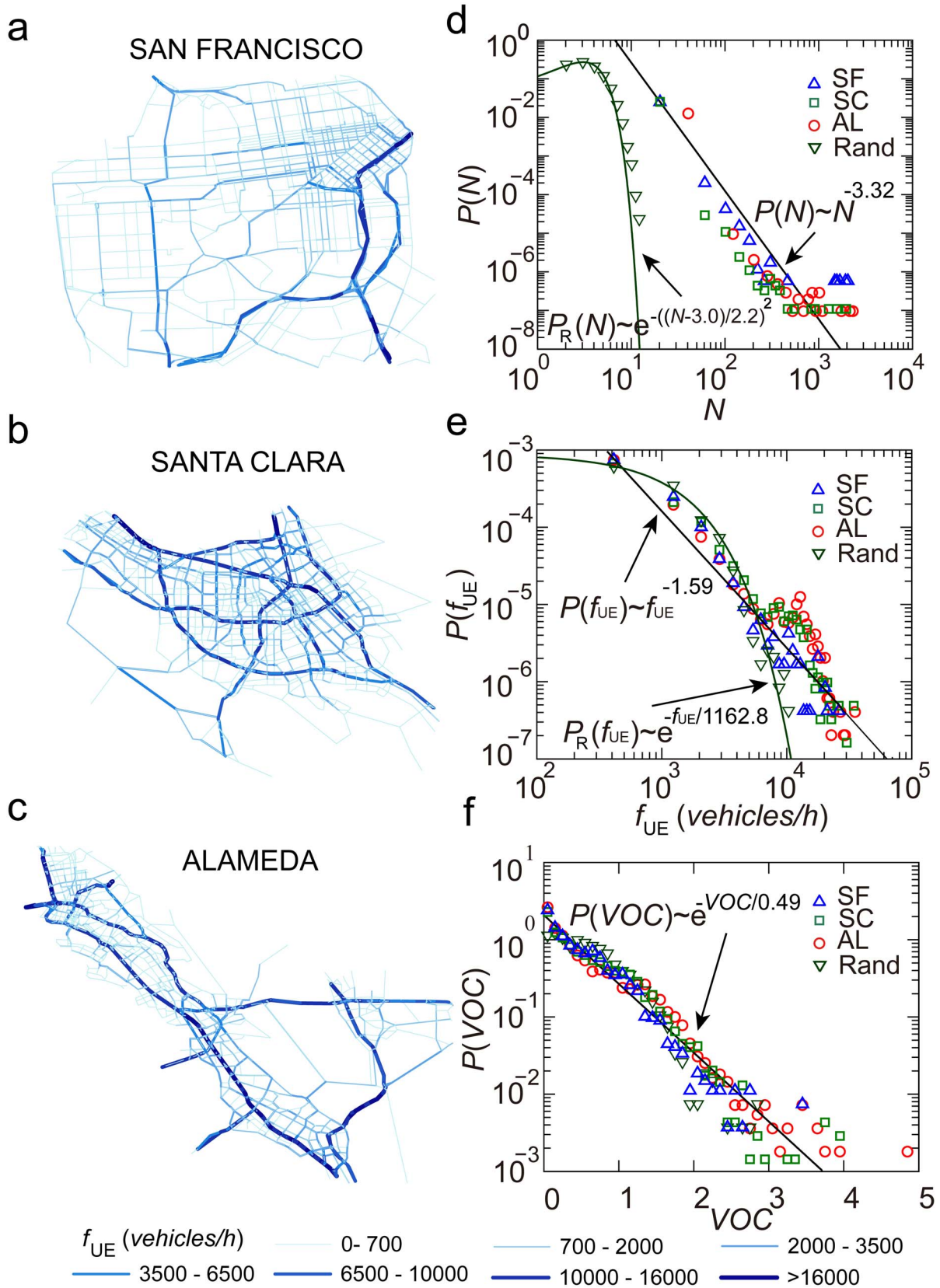


**Figure 3. Statistical analysis of traffic flow and volume over capacity (VOC).** (a), (b), (c) Spatial distributions of traffic flow are shown for San Francisco (SF), Santa Clara (SC), and Alameda (AL). (d) The number of trips between a pair of origin and destination. (e) Traffic flow  $f_{UE}$  was estimated using the actual ODs and the random OD. (f) VOC was estimated using the four ODs. doi:10.1371/journal.pone.0111088.g003



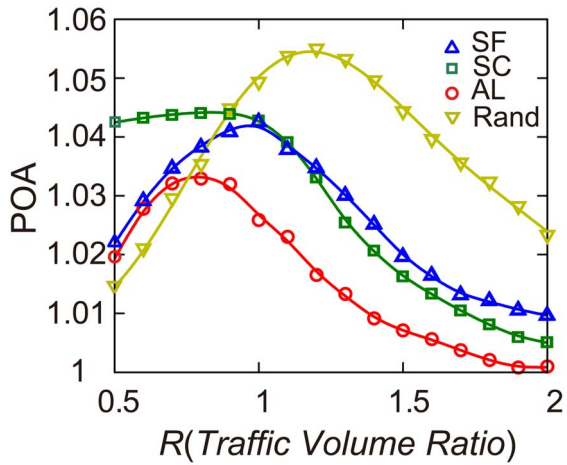


**Figure 4. Price of anarchy (POA) versus traffic volume ratio  $R$ .** Using actual travel demand distributions, the maximum POA=1.043 and POA=1.033 were observed at  $R=0.8$  for Santa Clara and Alameda. In San Francisco, the maximum POA estimated using actual travel demand distributions and random demand distributions were observed at  $R=1.0$  (POA=1.041) and  $R=1.2$  (POA=1.056) respectively. doi:10.1371/journal.pone.0111088.g004

pair of road intersections  $i$  and  $j$ . Travel time  $t_{ij}$  was estimated using the Bureau of Public Roads (BPR) function, which is widely used in civil engineering:

$$t_{ij}(f_{ij}) = t_f(1 + \alpha(f_{ij}/c_{ij})^\beta) \quad (4)$$

Here,  $c_{ij}$  is the capacity of the road segment from road intersection  $i$  to road intersection  $j$ . Commonly used values  $\alpha=0.15$  and  $\beta=4$  were selected [25]. The equilibrium flows  $f_{UE}$  were then numerically calculated using the Frank-Wolfe algorithm (see Method S1) toolkit provided by TransCAD 5.0, a transportation planning software [25,32].

Under the SO scenario, the socially optimal traffic flows  $f_{SO}$  were estimated by minimizing total travel time in Eq. (5):

$$T_{SO} = \sum f_{ij} t_{ij}(f_{ij}) \quad (5)$$

To calculate the socially optimal flow  $f_{SO}$ , the function of travel time was converted to the following:

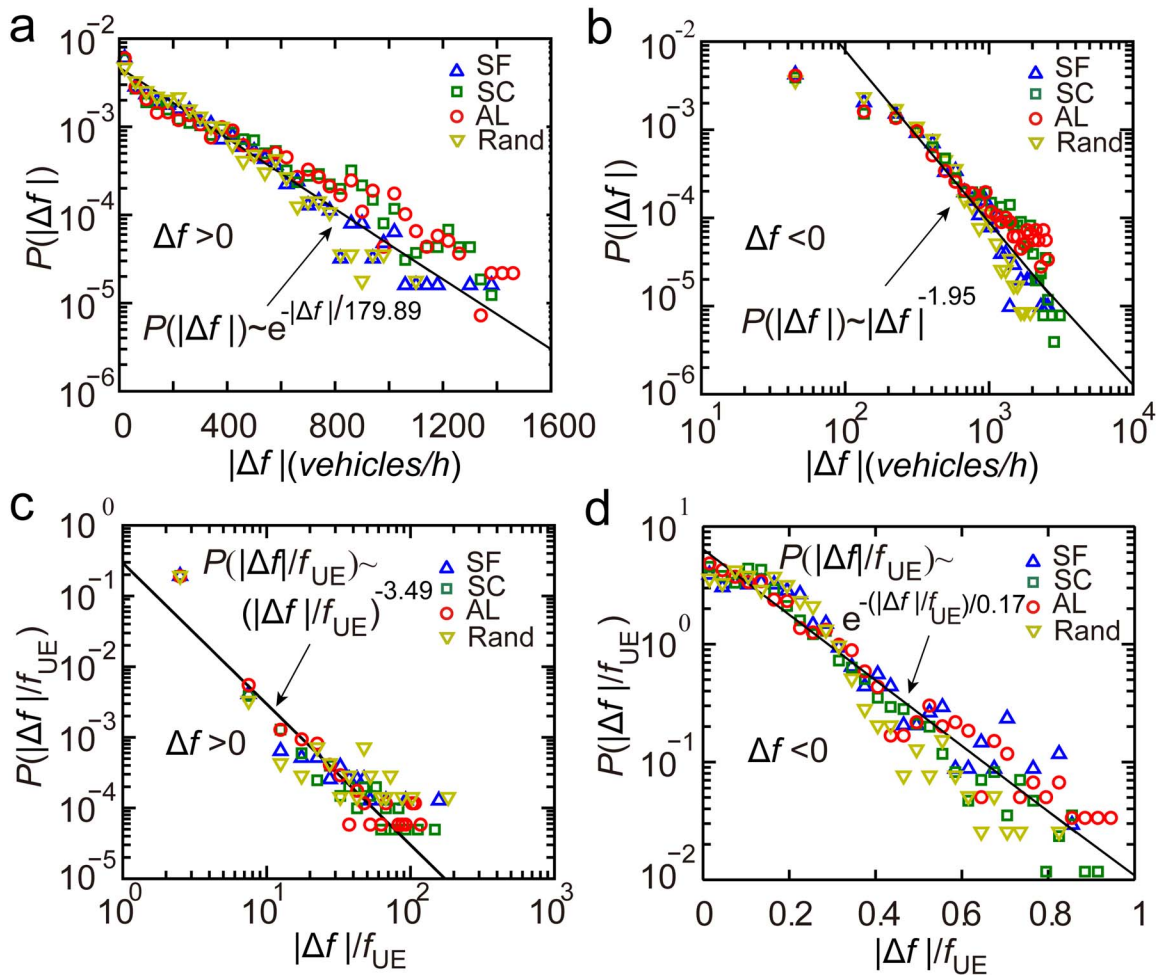


**Figure 5. Difference between equilibrium flow  $f_{UE}$  and socially optimal flow  $f_{SO}$ .** (a), (b) The difference between equilibrium flow and socially optimal flow  $|\Delta f|$  in the cases of  $\Delta f > 0$  and  $\Delta f < 0$ . (c), (d) The rescaled difference between equilibrium flow and socially optimal flow  $|\Delta f|/f_{UE}$  in the cases of  $\Delta f > 0$  and  $\Delta f < 0$ . doi:10.1371/journal.pone.0111088.g005

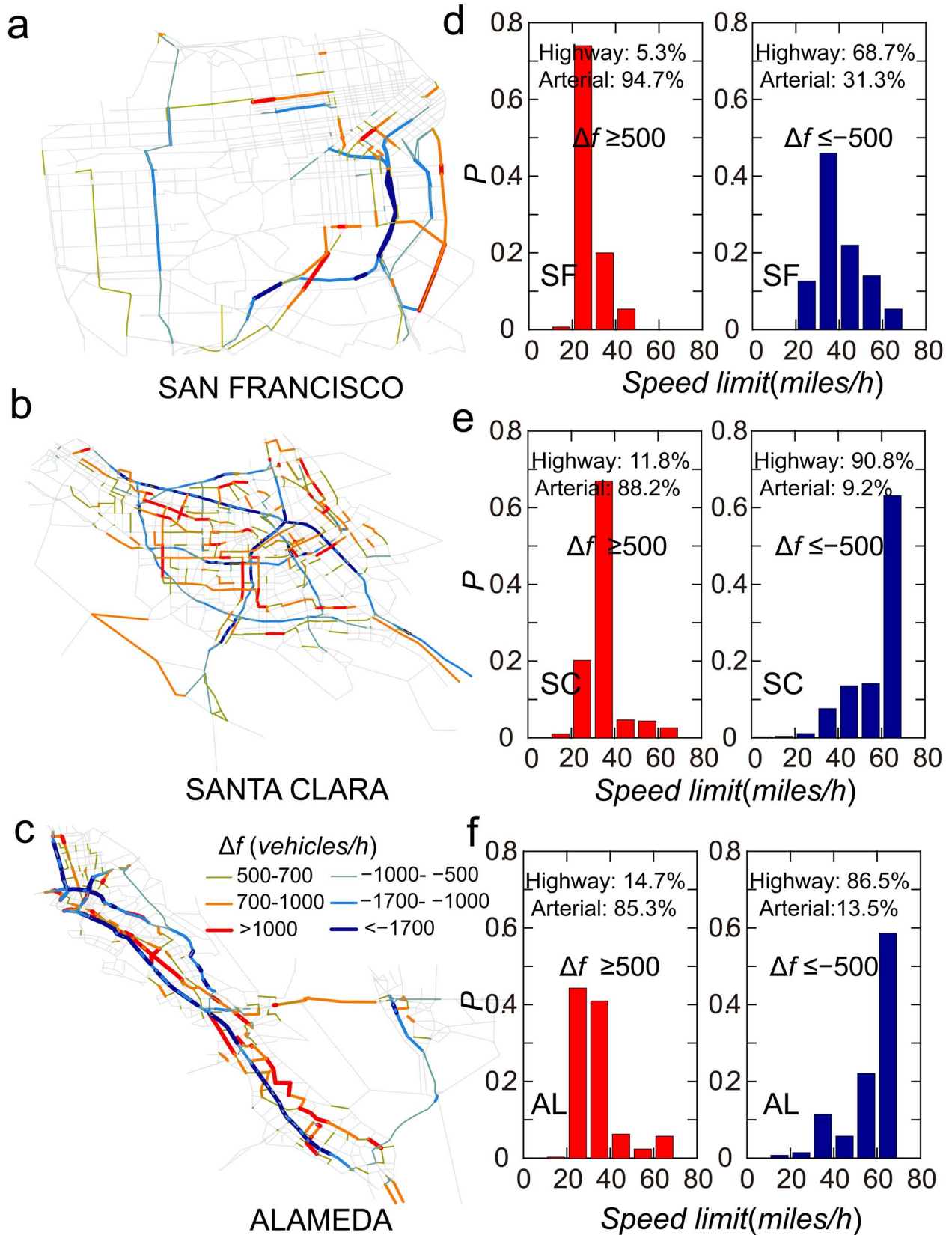


**Figure 6. Illustration of road segments with large  $|\Delta f|$ .** (a), (b), (c) Road segments with  $\Delta f \geq 500$  (vehicles/hour) and road segments with  $\Delta f \leq -500$  (vehicles/hour) in San Francisco, Santa Clara, and Alameda. (d), (e), (f) Speed limits of road segments with  $\Delta f \geq 500$  (vehicles/hour) and  $\Delta f \leq -500$  (vehicles/hour) in San Francisco, Santa Clara, and Alameda.  
 doi:10.1371/journal.pone.0111088.g006

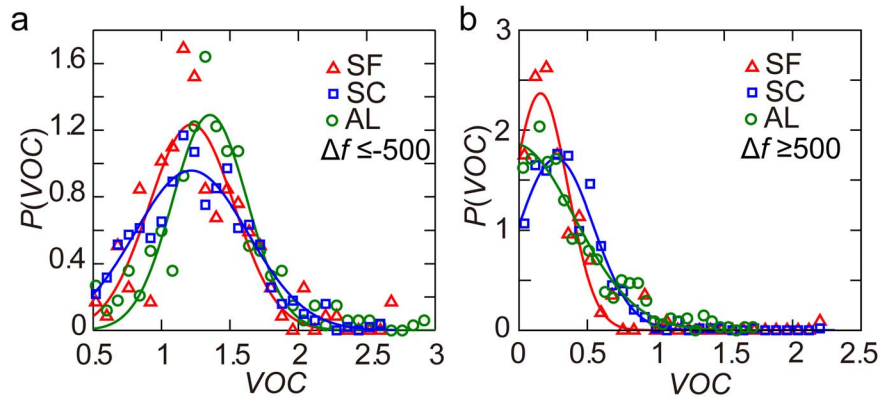


**Figure 7. Volume over capacity (VOC) of road segments with large  $|\Delta f|$ .** (a) VOC of road segments with  $\Delta f \leq -500$  (vehicles/hour) can be approximated by Gaussian distributions  $P(VOC) = ae^{-((VOC-b)/c)^2}$  with  $a = 1.24$  (0.96, 1.29),  $b = 1.22$  (1.22, 1.35),  $c = 0.44$  (0.59, 0.38), and  $R^2 = 0.80$  (0.92, 0.89) for San Francisco (Santa Clara, Alameda). (b) VOC of road segments with  $\Delta f \geq 500$  (vehicles/hour) can be approximated by Gaussian distributions  $P(VOC) = ae^{-((VOC-b)/c)^2}$  with  $a = 2.37$  (1.72, 1.86),  $b = 0.16$  (0.27, -0.04),  $c = 0.28$  (0.39, 0.62), and  $R^2 = 0.95$  (0.97, 0.95) for San Francisco (Santa Clara, Alameda).  
doi:10.1371/journal.pone.0111088.g007

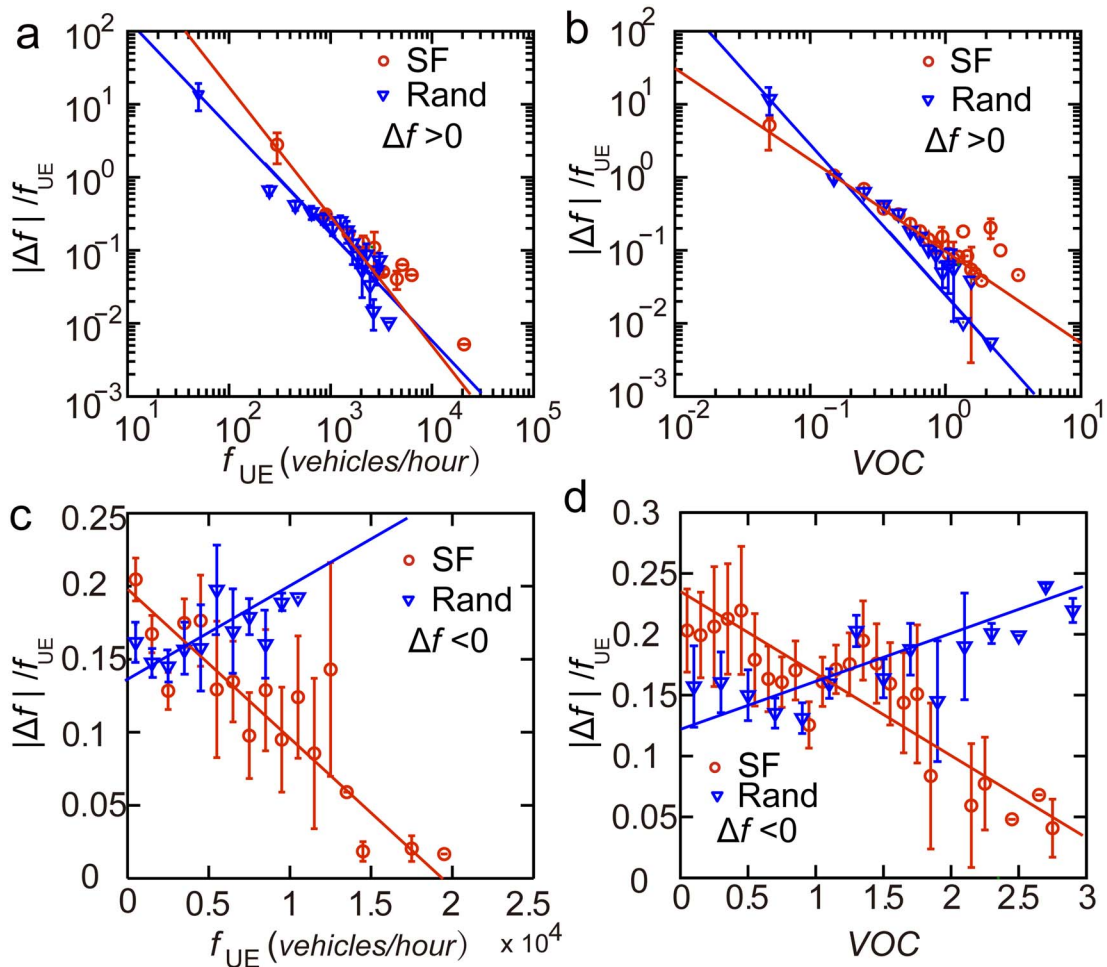


**Figure 8. The magnitude of traffic flow adjustment for reducing POA.** (a), (b) When increasing traffic flow of a road segment to reduce POA ( $\Delta f > 0$ ),  $|\Delta f|/f_{UE}$  can be approximated by two power-law functions  $|\Delta f|/f_{UE} = 8.18 \times 10^4 f_{UE}^{-1.81}$  ( $R^2 > 0.99$ ) or  $|\Delta f|/f_{UE} = 0.09 VOC^{-1.34}$  ( $R^2 > 0.99$ ). (c), (d) When decreasing traffic flow of a road segment to reduce POA ( $\Delta f < 0$ ),  $|\Delta f|/f_{UE}$  can be approximated by  $|\Delta f|/f_{UE} = -1.03 \times 10^{-5} f_{UE} + 0.20$  ( $R^2 = 0.83$ ) and  $|\Delta f|/f_{UE} = -0.06 VOC + 0.23$  ( $R^2 = 0.80$ ). Error bar here represents a 95% confidence interval.  
doi:10.1371/journal.pone.0111088.g008

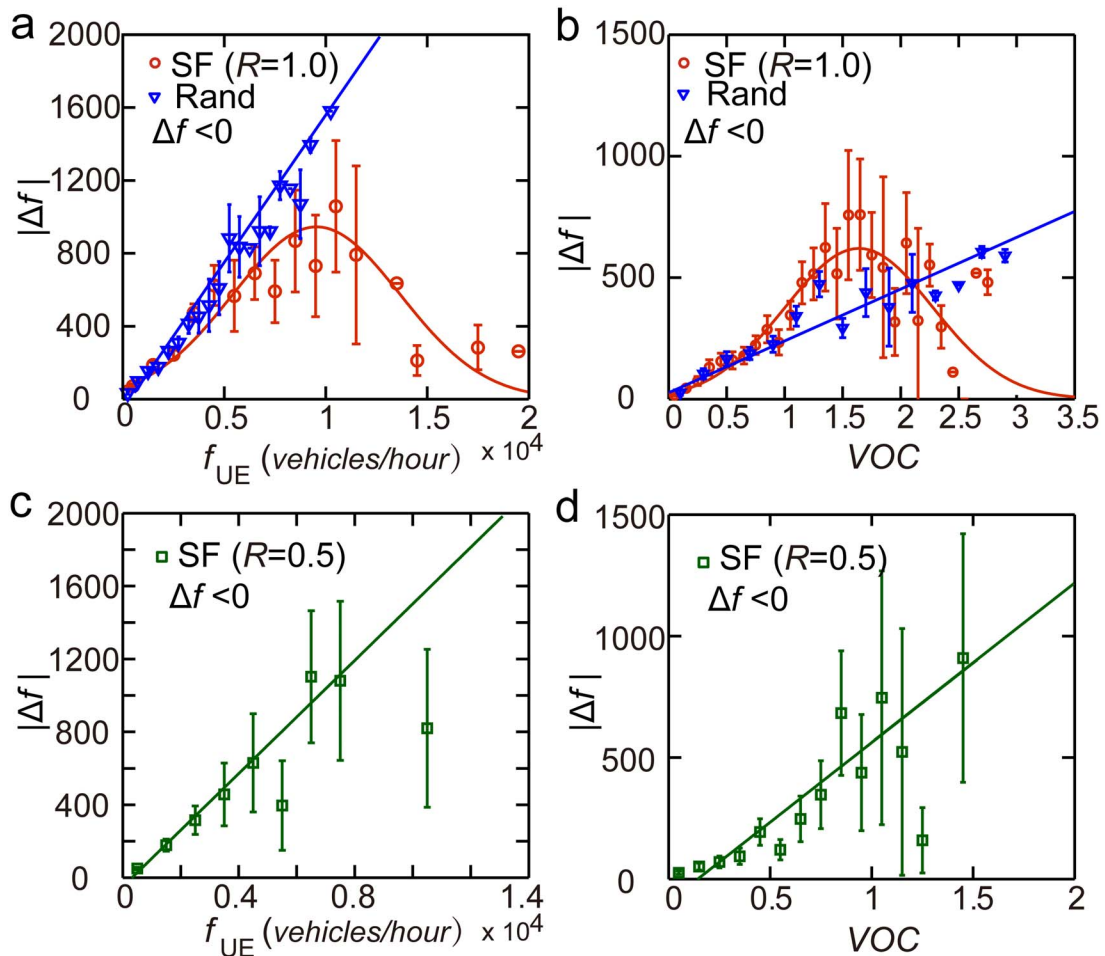


**Figure 9. The distribution and volume of travel demand determines the adjustment of traffic flow.** (a), (b)  $\Delta f$  estimated using the San Francisco random OD and actual OD show different correlations with  $f_{UE}$  and  $VOC$ . Statistical fits  $|\Delta f| = 0.15f_{UE} - 7.9$  ( $R^2 > 0.99$ ),  $|\Delta f| = 923e^{-(f_{UE} - 9805)/5683}$  ( $R^2 = 0.91$ ),  $|\Delta f| = 214.3VOC + 23.0$  ( $R^2 = 0.87$ ) and  $|\Delta f| = 630.7e^{-(VOC - 1.7)/0.8}$  ( $R^2 = 0.94$ ) were plotted to guide the eyes. (c), (d)  $|\Delta f|$  estimated using the re-scaled ( $R = 0.5$ ) San Francisco actual OD. Statistical fits  $|\Delta f| = 0.16f_{UE} - 49.6$  ( $R^2 = 0.89$ ) and  $|\Delta f| = 655.2VOC - 93.4$  ( $R^2 = 0.91$ ) were plotted to guide the eyes. Error bar here represents a 95% confidence interval. doi:10.1371/journal.pone.0111088.g009

$$\tilde{t}_{ij}(f_{ij}) = t_{ij}(f_{ij}) + f_{ij} \frac{dt_{ij}(f_{ij})}{df_{ij}} \quad (6)$$

Computing the integral of  $\tilde{t}_{ij}(f_{ij})$ , the following was determined:

$$\int_0^{f_{ij}} \tilde{t}_{ij}(\omega) d\omega = \int_0^{f_{ij}} [t_{ij}(\omega) + \omega \frac{dt_{ij}(\omega)}{d\omega}] d\omega \quad (7)$$

$$= \int_0^{f_{ij}} d[t_{ij}(\omega)\omega] = f_{ij}t_{ij}(f_{ij})$$

$$T_{SO} = \sum \int_0^{f_{ij}} \tilde{t}_{ij}(f) df \quad (8)$$

In this way, equation (7) possesses the same form as equation (3). Traffic flow  $f_{SO}$  can also be numerically calculated using the

Frank-Wolfe algorithm toolkit with the travel time function  $\tilde{t}_{ij}(f_{ij})$  (Eq. (6)).

## Results

Experimental tests show that humans find paths within networks in the perspective of minimizing their own travel costs [33,34]. For this reason, the equilibrium flow  $f_{UE}$  was used to analyze road usage patterns (Figure 3a-c). As Figure 3e shows that the equilibrium flow  $f_{UE}$  can be well approximated by a power-law distribution  $P(f_{UE}) = 10.5f_{UE}^{-1.59}$  for San Francisco, Santa Clara, and Alameda, indicating that road usages are similar and heterogeneous in the three counties ( $R^2 = 0.99$ ). Traffic flow for more than 80% of the road segments was below 2,000 (vehicles/hour), and there were 1.0%, 3.4%, and 5.6% of the road segments in San Francisco, Santa Clara, and Alameda having their  $f_{UE} > 10,000$  (vehicles/hour). The equilibrium flow  $f_{UE}$  was also measured using the random OD of San Francisco and observed to follow an exponential distribution  $P(f_{UE}) \sim e^{-f_{UE}/1,162.8}$  (Figure 3e). This indicates a much faster decay.

The volume over capacity  $VOC = f_{UE}/C$  was also measured ( $C$  is the capacity of a road segment). As shown in Figure 3f,  $VOC$



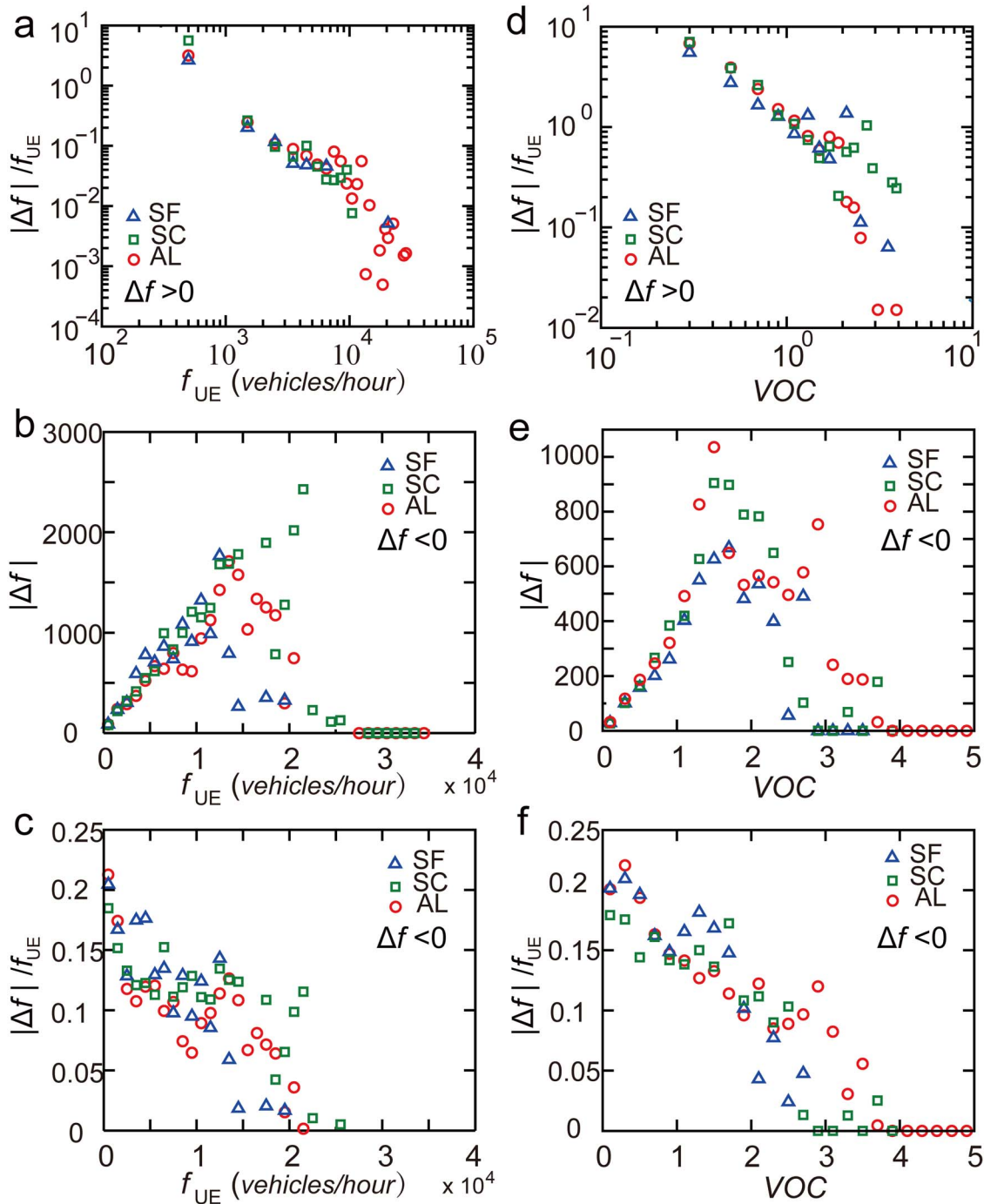


**Figure 10. The magnitude of traffic flow adjustment for reducing POA in the three counties.** (a)  $|\Delta f|/f_{UE}$  versus  $f_{UE}$  when  $\Delta f > 0$ . (b)  $|\Delta f|$  versus  $f_{UE}$  when  $\Delta f < 0$ . (c)  $|\Delta f|/f_{UE}$  versus  $f_{UE}$  when  $\Delta f < 0$ . (d)  $|\Delta f|/f_{UE}$  versus  $VOC$  when  $\Delta f > 0$ . (e)  $|\Delta f|$  versus  $VOC$  when  $\Delta f < 0$ . (f)  $|\Delta f|/f_{UE}$  versus  $VOC$  when  $\Delta f < 0$ . doi:10.1371/journal.pone.0111088.g010

estimated using either the actual ODs or the random OD can be approximated using an exponential distribution  $P(VOC) = 2.04e^{-2.04VOC}$  ( $R^2 = 0.98$ ), showing traffic flow in most road segments to be well within the roads' capacities, but there was a small number of congested road segments.

To determine how varying traffic volumes (total number of trips) affect POA, traffic volume ratio  $R$  was defined as the potential traffic volume over the current traffic volume. Traffic

volumes of the actual ODs and the random OD were scaled up or down using parameter  $R$ , at the same time the original distributions of travel demands were kept. As shown in Figure 4, the maximum POA = 1.043 and POA = 1.033 were both observed at  $R = 0.8$  in Santa Clara and Alameda, and the maximum POA estimated using actual distribution of travel demand was 1.041 in San Francisco when  $R = 1.0$  (Table S3). All of the POA first increased with  $R$  and then decreased with  $R$ , suggesting that the traffic flow patterns are similar under UE and SO scenarios when

traffic volume is very small or very large. This validates the generality of the findings obtained in [11]. Because when employing more-detailed travel demand information and road network information, similar pattern of POA versus traffic volume was still observed.

In Figure 4, the random OD of San Francisco was used to show how distribution of travel demand determines the POA. Unlike the maximum POA, which was predicted using the actual OD, a larger maximum POA = 1.056 was observed at a larger traffic volume ratio  $R = 1.2$ . POA was estimated using the actual OD and the random OD, which were 1.021 and 1.015, respectively, for small values of  $R$ , such as  $R = 0.5$ . They were 1.01 and 1.023, respectively, for large values of  $R$ , such as  $R = 2.0$ . The different patterns observed for POA versus  $R$  in these three counties also confirm that the distribution of travel demand needs to be considered in estimating the price of anarchy.

Given the huge traffic volumes in urban areas, a small POA can still mean a big loss of transport efficiency. Taking San Francisco as an example (POA = 1.041), drivers' selfish routing produced 1073.3 hours more travel time during only one hour of the morning rush. To offer guidance to reduce POA in urban road networks, the differences in equilibrium flow and socially optimal flow  $\Delta f = f_{SO} - f_{UE}$  were measured for each road segment. Results showed  $|\Delta f|$  to be heterogeneously distributed in the road networks ( $|\Delta f| = \Delta f$  when  $\Delta f > 0$  and  $|\Delta f| = -\Delta f$  when  $\Delta f < 0$ ). Most road segments have a small  $|\Delta f|$  and a few road segments, the targets of urban traffic controls, have  $|\Delta f|$  values as large as 3,000 (vehicles/hour). In the three counties, distributions of  $|\Delta f|$  can be approximated by an exponential distribution  $P(|\Delta f|) \sim e^{-|\Delta f|/179.9}$  ( $R^2 = 0.88$ ) when  $\Delta f > 0$  and by a power-law distribution  $P(|\Delta f|) \sim |\Delta f|^{-1.95}$  ( $R^2 = 0.98$ ) when  $\Delta f < 0$  (Figure 5a and b). The rescaled traffic flow difference  $|\Delta f|/f_{UE}$ , which quantifies the relative difference between  $f_{SO}$  and  $f_{UE}$ , can be approximated by a power-law distribution  $P(|\Delta f|/f_{UE}) \sim (|\Delta f|/f_{UE})^{-3.49}$  ( $R^2 > 0.99$ ) when  $\Delta f > 0$  and by an exponential distribution  $P(|\Delta f|/f_{UE}) \sim e^{-(|\Delta f|/f_{UE})/0.17}$  ( $R^2 = 0.88$ ) when  $\Delta f < 0$  (Figure 5c and d).

The heterogeneously distributed  $\Delta f$  suggests that traffic flow in only a small number of roads requires considerable adjustment. We found only 5.3% of the road segments in San Francisco, 9.3% of those in Santa Clara, and 9.8% of those in Alameda had  $\Delta f \geq 500$  (vehicles/hour) or  $\Delta f \leq -500$  (vehicles/hour) (Figure 6a–c, Table S3). In San Francisco, Santa Clara, and Alameda, 94.7%, 88.2%, and 85.3% of the road segments with  $\Delta f \geq 500$  (vehicles/hour) are arterial roads, and 68.7%, 90.8%, and 86.5% of the road segments with  $\Delta f \leq -500$  (vehicles/hour) are highways (Figure 6d–f). Targeted highways can noticeably reduce travel time, so they attracted large amounts of traffic and were overly used (most of them had  $VOC > 1.0$ ) (Figure 7a). Targeted arterial roads near the targeted highways may be suitable as alternative paths, but they do not see as much use as they could (most of them had  $VOC < 1.0$ ) (Figure 7b). The present findings held true for all the three counties, indicating a general explanation for the price of anarchy in road networks. These results can provide insight that can be used to identify roads in need of traffic control in practical situations.

We next explored the magnitude of traffic flow adjustment to reduce POA. Taking San Francisco as an example, when increasing traffic flow of a road segment ( $\Delta f > 0$ ), the rescaled difference of traffic flows  $|\Delta f|/f_{UE}$  can be approximated by power-law functions  $|\Delta f|/f_{UE} \sim f_{UE}^{-1.81}$  and  $|\Delta f|/f_{UE} \sim VOC^{-1.34}$ . This offers a guidance for increasing traffic flow in the targeted road segments when their  $f_{UE}$  or  $VOC$  is known (Figure 8a and b). The

increase of traffic flow in congested roads or roads with large traffic would be very tiny. Obvious increases in traffic flow were only observed in roads with low  $f_{UE}$  and  $VOC$ . This law also holds for the case of the random OD.

When decreasing traffic flow of a road segment to reduce POA ( $\Delta f < 0$ ), the rescaled difference of traffic flows  $|\Delta f|/f_{UE}$  can be approximated by linear functions  $|\Delta f|/f_{UE} = -1.03 \times 10^{-5} f_{UE} + 0.20$  ( $R^2 = 0.83$ ) and  $|\Delta f|/f_{UE} = -0.06 VOC + 0.23$  ( $R^2 = 0.80$ ) (Figure 8c and d). However, for the case of the random OD, different functional relationship was found,  $|\Delta f|/f_{UE}$  was observed to increase linearly with  $f_{UE}$  and  $VOC$  (Figure 8c and d).

To understand the observed different relationships between  $|\Delta f|/f_{UE}$  and  $f_{UE}$  ( $VOC$ ), we analyzed the traffic flow difference  $|\Delta f|$  for the case of the random OD and the case of the actual OD. We found that  $|\Delta f|$  estimated using the random OD increased linearly with  $f_{UE}$  and  $VOC$ . However, counter intuitively,  $|\Delta f|$  estimated using the actual OD first increased and then decreased with  $f_{UE}$  and  $VOC$ . The roads with the largest flow or  $VOC$  were not those requiring the highest reduction of traffic. The highest reduction of traffic flow was observed at intermediate values of  $f_{UE} \sim 9,805$  (vehicles/h) and  $VOC \sim 1.7$  (Figure 9a and b).

The counter intuitive result could be resulted from the different distributions of traffic flow estimated by the random OD and the actual OD. Comparing with the case of the random OD, traffic flow estimated using the actual OD was more heterogeneously distributed. There are much more road segments with large traffic flow (Figure 3e), preventing drivers from selfishly switching routes. This phenomenon is similar to that when traffic volume is very large, traffic flow patterns under UE scenario and SO scenario are similar (POA  $\sim 1.0$ ). To further test this explanation, the actual ODs were scaled down using parameter  $R = 0.5$ , the observed maximum traffic flow is largely reduced. As Figure 9c and d shows, the difference in traffic flow  $|\Delta f|$  shows similar pattern with the case of the random OD rather than the case of the actual OD.

We further analyzed the magnitude of traffic flow adjustment for reducing POA for Santa Clara and Alameda. Similar functional relationships between  $|\Delta f|/f_{UE}$  and  $f_{UE}$ ,  $VOC$  were observed (Figure 10). The significance of these findings is that it offered useful guidance that could reduce POA for urban road networks, using traffic flow  $f_{UE}$  only. This was widely available and recorded by many devices.

## Conclusions

To conclude, we generate morning-peak commute ODs for three Bay Area counties and study the price of anarchy using actual travel demand in large-scale road networks. The different patterns observed for POA versus  $R$  in the three counties showed that both volume and distribution of travel demand determine the POA in a road network. The difference of equilibrium flow and socially optimal flow  $|\Delta f|$  was measured for each road segment. It was found that  $|\Delta f|$  for most roads is tiny. For this reason, adjusting traffic flow of a small number of roads can push a system toward its social optimum. Here, roads with large  $|\Delta f|$  were found to be only a few highways that saw excessive use due to their high speed limits and the neighboring arterial roads, which can offer alternative paths. The rescaled traffic flow difference  $|\Delta f|/f_{UE}$  was found to have power-law functional relationships with  $f_{UE}$  and  $VOC$  when  $\Delta f > 0$  and have linear functional relationships with  $f_{UE}$  and  $VOC$  when  $\Delta f < 0$ . Surprisingly, the roads with the largest traffic flow and  $VOC$  did not have the largest adjustment of traffic flow.

The present work can inform specific intervention strategies on reducing the loss of efficiency caused by agents' selfish routing in

urban road networks, a crucial infrastructure that billions of people use every day. The present work uses real-world travel demand data to explore the way to reduce POA. The elucidation of these findings may draw more attention to the use of actual transport demand information in the optimal control of a broad set of networks experiencing a lack of coordination among agents.

## Supporting Information

**Figure S1 Distributions of lengths and free travel times of road segments.** Both lengths and free travel times of road segments follow similar distributions in three counties. (PDF)

**Figure S2 Vehicle usage rates (*VUR*) in census tracts.** Different colors represent different vehicle usage rates. Urban areas have lower *VUR* than suburban areas. (PDF)

**Figure S3 Illustration of census tracts and convention from census tract based OD to intersection based OD.** The road segments in the vicinity of San Francisco downtown are depicted by gray lines and the small black dots are the road intersections that lie in the census tracts inside. (PDF)

## References

- Brockmann D, Hufnagel L, Geisel T (2006) The scaling laws of human travel. *Nature* 439: 462–465.
- González MC, Hidalgo CA, Barabási AL (2008) Understanding individual human mobility patterns. *Nature* 435: 779–782.
- Song C, Qu Z, Blumm N, Barabási AL (2010) Limits of predictability in human mobility. *Science* 327: 1018–1021.
- Helbing D (2003) A section-based queueing-theoretical traffic model for congestion and travel time analysis in networks. *J. Phys. A: Math. Gen.* 36: 593–598.
- Schrank D, Lomax T (2009) Annual urban mobility report (Texas Transportation Institute). <http://mobility.tamu.edu/ums/>.
- Chin ATH (1996) Containing air pollution and traffic congestion: transport policy and the environment in Singapore. *Atmospheric Environment* 30(5): 787–801.
- Rosenlund M, Forastiere F, Stafoggia M, Porta D, Perucci M, et al (2008) Comparison of regression models with land-use and emissions data to predict the spatial distribution of traffic-related air pollution in Rome. *Journal of Exposure Science and Environmental Epidemiology* 18: 192–199.
- Du WB, Wu ZX, Cai KQ (2013) Effective usage of shortest paths promotes transportation efficiency on scale-free networks. *Physica A* 392(17): 3505–3512.
- Wang P, Hunter T, Bayen AM, Schechtner K, González MC (2012) Understanding the road usage patterns in urban areas. *Scientific Reports* 2: 1001.
- Wu Z, Braunstein LA, Havlin S, Stanley HE (2006) Transport in weighted networks: partition into superhighways and roads. *Phys. Rev. Lett.* 96: 148702.
- Youn H, Gastner MT, Jeong H (2008) Price of anarchy in transportation networks: efficiency and optimality control. *Phys. Rev. Lett.* 12(101): 0712–1598.
- Roughgarden T (2005) *Selfish routing and the price of anarchy*. Cambridge, USA: MIT Press.
- Roughgarden T (2006) On the severity of Braess's Paradox: Designing networks for selfish users is hard. *Journal of Computer and System Sciences* 72: 922–953.
- Nagurney A (2010) The negation of the Braess's paradox as demand increases: The wisdom of crowds in transportation networks. *EPL* 91(4): 48002.
- Koutsoupias E, Papadimitriou C (1999) Worst-case equilibria. *STACS 99* Springer Berlin Heidelberg: 404–413.
- Barthélemy M, Flammini A (2008) Modeling urban streets patterns. *Phys. Rev. Lett.* 100: 138702.
- Crucitti P, Latora V, Porta S (2006) Centrality measures in spatial networks of urban streets. *Phys Rev E* 73: 036125.
- Yan G, Zhou T, Hu B, Fu ZQ, Wang BH (2006) Efficient routing on complex networks. *Phys. Rev. E.* 73: 046108.
- Jiang B, Zhao S, Yin J (2008) Self-organized natural roads for predicting traffic flow: a sensitivity study. *J Stat Mech*: P07008.
- Kurant M, Thiran P (2006) Layered complex networks. *Phys. Rev. Lett.* 96: 138701.
- Liu C, Du WB, Wang WX (2014) Particle Swarm Optimization with Scale-Free Interactions. *PLoS one* 9(5): e97822.
- Acemoglu D, Johari R, Ozdaglar A (2007) Partially Optimal Routing. *IEEE Journal on selected areas in communications* 25(6): 1148–1160.
- Navteq Official website. Available: <http://www.navteq.com/>. Accessed 2014 Oct 5.
- US Census Bureau website. Available: [http://www.census.gov/geo/www/tiger/tgrshp2010/tgrshp20\\_10.html](http://www.census.gov/geo/www/tiger/tgrshp2010/tgrshp20_10.html). Accessed 2014 Oct 5.
- Caliper website. Available: <http://www.caliper.com/PDFs/TravelDemandModelingBrochure.pdf>. Accessed 2014 Oct 5.
- National TDM and Telework Clearinghouse website. Available: <http://www.nctr.usf.edu/clearinghouse/censusavo.htm>. Accessed 2014 Oct 5.
- Bureau of Transportation Statistics website. Available: [http://www.rita.dot.gov/bts/sites/rita.dot.gov/bts/files/subject\\_areas/national\\_household\\_travel\\_survey/index.html](http://www.rita.dot.gov/bts/sites/rita.dot.gov/bts/files/subject_areas/national_household_travel_survey/index.html). Accessed 2014 Oct 5.
- Seto YW, Holt A, Rivard T, Bhatia R (2007) Spatial distribution of traffic induced noise exposures in a US city: an analytic tool for assessing the health impacts of urban planning decisions. *International Journal of Health Geographics* 6: 24.
- Dijkstra EW (1959) A note on two problems in connexion with graphs. *NumerischeMathematik* 1: 269–271.
- Nathan H Gartner (1980) Optimal traffic assignment with elastic demands: a review part ii. algorithmic approaches. *Transportation Research* 14(2): 192–208.
- Beckmann MJ, Meguire CR, Winsten CB (1956) *Studies in the economics of transportation*. New Haven, USA: Yale University Press.
- LeBlanc LJ, Morlok EK, Pierskalla WP (1975) An efficient approach to solving the road network equilibrium traffic assignment problem. *Transportation Research* 9(5): 309–318.
- Selten R, Chmura T, Pitz T, Kube S, Schreckenberg M (2007) Commuters route choice behaviour. *Games and Economic Behavior* 58(2): 394–406.
- Stein WE, Rapoport A, Scale DA, Zhang H, Zwick R, et al. (2007) Batch queues with choice of arrivals: Equilibrium analysis and experimental study. *Games and Economic Behavior* 59(2): 345–363.